A Framework for Numerical Simulation of Turbulent Incompressible Unsteady Flame Dynamics Coupled with Acoustic Calculations in Time And Frequency Domains

S. R. Chakravarthy*[1], C. Balaji[2], R. K. R. Katreddy[1], A. Nath[3]

[1] Department of Aerospace Engineering, Indian Institute of Technology Madras
Sardar Patel road, Kanagam, 600036 and Chennai, India
[2] Metacomp Technologies
Chennai, India
[3] CD-ADAPCO
Bangalore, India
* Corresponding author: src@ae.iitm.ac.in

A generalized formulation of combustion-acoustic coupling at simultaneous multiple time- and length-scales is presented. The scale separation is applied to the compressible NavierStokes equations, and the flow quantities are expanded about the mean flow Mach number. This results in equations separating into the one governing the combustion at shorter length/longer time-scale, and the other, the acoustics at longer length/shorter time-scale. Explicit coupling terms, the dilatation of the base flow as a source of acoustic energy and the acoustic Reynolds stress (ARS) as the source to base flow momentum are identified. Simulations are carried out in a dump combustor, under laminar flow conditions as a model problem, and under turbulent conditions as in real cases. The turbulent flow is simulated by large eddy simulation (LES) and unsteady Reynolds-averaged Navier-Stokes (URANS) approach. Additional turbulent-acoustic interaction terms are identified in the decomposition and are modeled. The results show good agreement with experimental data.

1 Introduction

Combustion instability in aero and power generating gas turbines has been a long-standing problem. Some of the significant mechanisms of combustion instability involve vortex shedding [1] and equivalence ratio fluctuations [2], both leading to heat release rate fluctuations. Typically, combustion instability is experimentally investigated during conditions of high amplitude excitation of sound, to evaluate the phase relationship between the different processes– vortex shedding, fuel inflow fluctuations, heat release rate, and acoustic pressure and/or velocity– all occurring at the same time scale. Sivasegaram and Whitelaw [3] distinguished the dominant frequencies and amplitudes under contrasting conditions of "rough" and "smooth" combustion. Lieuwen [4] showed the rise of acoustic pressure amplitude from low levels to limit cycle as either subcritical

or supercritical bifurcations. Chakravarthy et al. [5] have presented a map of onset of instability by varying the conditions widely from those of low amplitude noise excitation to high amplitude discrete tones. The map is based on the ratio of flow to acoustic time scales, and clearly brings out the approach of the two time scales during combustion instability in the form of an inverse flow-acoustic lock-on, wherein the duct acoustics locks on to the vortex shedding. Balachandran et al. [6] have shown that the flame distinctly changes its structure from an elongated diffusion flame to a highly compact premixed flame, with the fuel injection close to the flame holder.

The classical theoretical approach in solving combustion instability is within an acoustic framework, wherein the acoustics is modelled in the harmonic domain with sources obtained from the combustion field, usually the heat release rate fluctuations [7]. Often, the fluctuations in heat release rate are also modelled using localized response functions obtained from external perturbation of the flame evaluated separately. Wu et al. [8] attempted to model the details of the combustion zone along with the acoustic fluctuations by considering different length scales for the acoustic and hydrodynamic oscillations and the preheat and reacting zones of a premixed flame. Tyagi et al. [9] computed the flame oscillations in a small combustion zone with spatially uniform flow embedded in a larger acoustic zone, with the coupling between the two provided by the heat release rate from the former to the latter and the acoustic velocity and pressure from the latter to the former at each time instant. Balasubramanian and Sujith [10] have shown that the convective-diffusive process in fluid flow and combustion is non-normal, and it influences the acoustic behaviour in the same manner as well; hence, late-time stability of a thermoacoustic system could still involve a transient growth at earlier times. The use of compressible large eddy simulation (LES) in combination with acoustic analysis has been reported recently [11,12]. The bifurcation of the flame structure from a stable to unstable state with slight increase in the reactant temperature at the inlet is also simulated by LES [13].

Some of the above works on combustion instability have taken into account the disparity in the length scales of the combustion zone and the acoustic field, particularly under combustion instability conditions when the flame becomes highly compact. However, most works implicitly adopt an approach of equal time scales of the combustion and acoustic processes, which prevails mainly during combustion instability conditions. A realistic predictive approach of combustion instability, on the contrary, ought to consider the flow/combustion and the acoustics to occur at different time scales in general, and actually predict the set of operating conditions when the two time scales would indeed match, leading to combustion instability. Such an approach would also enable the simulation of how the flame approaches a compact structure as instability conditions are triggered from an initially steady state when the flame is relatively elongated.

An approach of the above kind warrants an explicit consideration of multiple length and time scales simultaneously prevailing in a combustor in general. Adopting multiple scales allows one to expand the fluid dynamic quantities typically in terms of the ratio of scales and decompose different sets of equations that govern the processes at the different scales. This has been adopted for multiple time scales but single length scale by Muller [14], and for single time scale but multiple length scales by Klien [15]. Muller [14] filters out the acoustic parts of the conservation equations and retains an average (acoustic) velocity tensor in the base flow's momentum balance as its net effect. Klein [15] points out the application of the single-time/multiple-length scale approach in thermoacoustics in general (not specifically combustion instability), but his major interest is in atmospheric flows.

In the present work, a simultaneous multiple time- and length-scale approach is adopted to investigate combustion instability in a generalized framework. The combustion zone is, in general, shorter than the acoustic zone for longitudinal acoustic modes, and the convective time scale in the combustion zone is larger than the acoustic time scale, since the mean Mach number of the flow is small. The simultaneous consideration of multiple scales in both time and space is handled by expressing both the ratio of length scales and the mean flow Mach number in terms of a common

small parameter [15], which enables the decomposition of the governing equations into nonlinear incompressible Navier-Stokes and linearized compressible Euler equations respectively for the combustion and acoustic zones. Additionally, each set of equations offers source terms to the other: the divergence of the base flow acts as an acoustic energy source in general, and the average acoustic velocity tensor acts as a source of base flow momentum. In the limit of equal time- or length-scales, the respective equation sets are retrieved. A model problem of 2D laminar nonpremixed flame in a dump combustor with temperature-dependent density is worked out with variation of the relevant parameters to illustrate the important features of the approach. It is observed that as the combustion-acoustic interaction evolves, the flame curls into an increasingly compact region that causes the flow and acoustic time scales to approach each other, leading to instability. The formulation is extended to 3D turbulent flames and the results are compared with experimental data.

2 Mathematical Formulation

The schematic of the problem with specific context to a dump combustor is shown in Fig. 1. The flow/combustion field is modelled in a shorter length scale h and longer (convective) time scale t = h/u, whereas the acoustics is modelled in a longer length scale L (for longitudinal acoustic modes) and shorter time scale τ = L/c. h is characteristic of the lateral dimensions of the combustor, such as the step height, and L is the length of the combustor. u and c are the reference flow and sound speeds. The fluid is considered to be a calorically perfect gas and all the diffusion coefficients are assumed equal and constant. The conservation equations are non-dimensionalised with shorter length and time scales, h and τ respectively [16]. Apart from other non-dimensional quantities, the resulting set of equations have M = u/c and h/L, the Mach number and the ratio of length scales respectively. Taken together, these constitute the simultaneous multiple length and time scales. Both of these quantities are taken to be small in the present formulation. To handle two small parameters simultaneously, each of them is in turn represented as a function of a single small number ϵ through the relations $M = \epsilon^m$ and $h/L = \epsilon^n$.

Any dependent variables ϕ is expanded according to the ansatz $\phi = \epsilon^i \, \phi_i$. Splitting the spatial and temporal derivatives for the two scales considered, expanding the variables as powers of ϵ and comparing equi-order terms in ϵ, we decompose the conservation equations for the flow and acoustics in their respective length and time scales. In the resulting set of equations, it is observed that both the flow and acoustics affect the fluid velocity to leading order. Further, temporally averaging the base-flow equations and spatially averaging the acoustic equations results in the definition of new velocity variables that can be identified distinctly with the base flow and the acoustics. This process also results in the appearance of explicit interaction terms between the base-flow and acoustics. The final sets of conservation equations for the flow and acoustics are given below [16]:

Flow:

$$\frac{\partial \rho_0}{\partial t} + \frac{\partial}{\partial x_j}(\rho_0 \overline{u_{0j}}^{\tau}) = 0 \tag{1}$$

$$\frac{\partial}{\partial t}(\rho_0 \overline{u_{0i}}^{\tau}) + \frac{\partial}{\partial x_j}(\rho_0 \overline{u_{0i}}^{\tau} \overline{u_{0j}}^{\tau}) + \frac{1}{\gamma}\left(\frac{\partial \overline{p_2}^{\tau}}{\partial x_i}\right) - \frac{1}{Re}\left(\frac{\partial^2 \overline{u_{0i}}^{\tau}}{\partial {x^2}_j} + \frac{1}{3}\frac{\partial}{\partial x_i}\left(\frac{\partial \overline{u_{0k}}^{\tau}}{\partial x_k}\right)\right) = -\frac{\partial}{\partial x_j}(\rho_0 \overline{u_{0i}'^{\tau} u_{0j}'^{\tau}}^{\tau}) \tag{2}$$

$$\frac{dp_0}{dt} + \gamma p_0 \frac{\partial \overline{u_{0j}}^{\tau}}{\partial x_j} = (\gamma - 1) Da Q_{R0} + \frac{\gamma}{Pe}\frac{\partial^2 T_0}{\partial {x^2}_j} \tag{3}$$

$$\frac{\partial \rho_{K0}}{\partial t} + \frac{\partial}{\partial x_j}(\rho_{K0} \overline{u_{0j}}^{\tau}) - \frac{1}{ReSc}\frac{\partial^2 \rho_{K0}}{\partial {x^2}_j} - Da_K \omega_K = 0 \tag{4}$$

$$p_0 = \rho_0 T_0 \tag{5}$$

Acoustics:

$$\frac{\partial \rho_1}{\partial \tau} + \frac{\partial}{\partial \xi_j}(\overline{\rho_0}^x u_0{}_j'^\tau) = -\frac{\partial}{\partial \xi_j}(\overline{\rho_0}^x \overline{\overline{u_{0j}}^\tau}^x + \overline{\rho_0{}'^x \overline{u_{0j}}^{\tau\prime x}}^x) \tag{6}$$

$$\overline{\rho_0}^x \frac{\partial u_{0i}'^\tau}{\partial \tau} + \frac{1}{\gamma}\frac{\partial p_1}{\partial \xi_i} = 0 \tag{7}$$

$$\frac{\partial p_1}{\partial \tau} + \gamma p_0 \frac{\partial u_{0i}'^\tau}{\partial \xi_j} = -\gamma p_0 \frac{\overline{\overline{u_{0j}}^\tau}^x}{\partial \xi_j} \tag{8}$$

$$\frac{\partial \overline{\rho_{K1}}^x}{\partial \tau} + \frac{\partial}{\partial \xi_j}(\overline{\rho_{K0}}^x u_0{}_j'^\tau) = -\frac{\partial}{\partial \xi_j}(\overline{\rho_{k0}}^x \overline{\overline{u_{0j}}^\tau}^x + \overline{\rho_{k0}{}'^x \overline{u_{0j}}^{\tau\prime x}}^x) \tag{9}$$

$$p_1 = \rho_1 \overline{T_0}^x + \overline{\rho_0}^x T_1 \tag{10}$$

In these equations, ρ_0, $\overline{u_{0j}}^\tau$, $\overline{p_2}^\tau$, ρ_{K0} and T_0 are base flow mixture density, velocity, pressure (hydrodynamic) and temperature respectively and ρ_1 ,$u_{0j}'^\tau$, p_1, ρ_{K1} and T_1 are the corresponding acoustic quantities. Re, Pe, Sc, Da and Da_K, are the Reynolds, Peclet, Schmidt, Damköhler and Damköhler for species K respectively. With these variables and non-dimensional quantities, (1)–(5) can be identified as the Navier-Stokes equations for incompressible flow with temperature-dependent density governing the combustion zone, and (6)–(10) as the linearized Euler equations governing the acoustic zone. Explicit coupling terms, viz, the flow divergence over acoustic length scale (RHS of (8)) and acoustic Reynolds stress (ARS, RHS of (2)) are brought out naturally without any ad-hoc treatment.

In this formulation, the acoustic damping does not show up. This is because, the length scale associated with the acoustic boundary layer where most of the damping occurs is not considered. Accounting for acoustic damping is important to predict the long-time behaviour of the system and eventually predict the limit cycle amplitude of the system. Towards this end, the above formulation is extended to include acoustic damping by considering a visco-thermal friction term [17].

Acoustic damping predominantly occurs near the walls in the acoustic boundary layer, whose length scales are considerably lower than the flow length scales; therefore their contribution is not brought out in the acoustic balance equations, (6-10). Considering the acoustic boundary layer in the solution will increase the computational cost considerably. Therefore, in order to explore the effect of damping in the evolution of the coupled system at reasonable computational cost, a visco-thermal friction term [17] is added to the acoustic momentum balance equation (7); the resultant equation is given below,

$$\overline{\rho_0}^x \frac{\partial u'^\tau{}_{0,i}}{\partial \tau} + \frac{1}{\gamma}\frac{\partial p_1}{\partial \xi_i} = -2\alpha \overline{\rho_0}^x u_{0i}{}'^\tau \tag{11}$$

where, α is the non-dimensional Helmholtz-Kirchhoff wall-attenuation coefficient [18], non-dimensionalized by the duct length L. In combustion flow fields, acoustic attenuation is increased due to the presence of water vapour [18]. This is approximately taken into account by increasing α up to twenty times the calculated value.

When the flow is turbulent, the range of flow scales span from the integral time/length to the Kolmogrov time/length scales. There are three possibilities that can arise in the position of the acoustic time scale relative to the turbulent spectrum. The acoustic time scale could be shorter than the Kolmogrov time scale, or it can be longer than the integral time scale, or it can lie in between these two scales. The first one occurs for short combustors and relatively low Re flows. The second possibility, occurs when the combustor is relatively long and the characteristic transverse dimension is short. These two possibilities are relatively rare in occurrence when compared to the third possibility. The most common candidate is the last possibility wherein the acoustic time scale falls in between the integral and Kolmogrov time scales. The approach taken to model turbulent flow is to introduce a new time scale. For example, LES resolves scales that are longer than the cut-off scale used in the spatial filtering. URANS method resolves the longest time scale (close to the integral time scale).

With LES, the temporal average taken over the acoustic time scale τ, which implicitly imposes a filter width Δ_a; the spatial grid should be fine enough to resolve this. The temporal average of the convective term in the flow momentum equation results in the cross-correlation of the temporal fluctuations, which can further be decomposed spatially as

$$\overline{u_{0i}{}'^{\tau} u_{0j}{}'^{\tau}}^{\tau} = \overline{\overline{u_{0i}{}'^{\tau}}^{x} \overline{u_{0j}{}'^{\tau}}^{x}}^{\tau} + \overline{u_{0i}{}'^{\tau\prime x} u_{0j}{}'^{\tau\prime x}}^{\tau} + \overline{\overline{u_{0i}{}'^{\tau}}^{x} u_{0j}{}'^{\tau\prime x}}^{\tau} + \overline{u_{0i}{}'^{\tau\prime x} \overline{u_{0j}{}'^{\tau}}^{x}}^{\tau} \qquad (12)$$

The first term is the ARS, but the other terms are subgrid scale stresses to be modelled. The second term refers primarily to turbulent fluctuations, but the last two terms indicate turbulence-acoustic interaction (TAI) terms.

In the case of URANS, the flow equations are Favre-averaged at the integral time scale. Since the flow equations are already averaged over the acoustic time scale which is lesser than the integral time scale, the turbulent Reynolds stress (TRS) term obtained in this case would be corresponding to turbulent fluctuations in between the two scales. However, the remaining term containing the acoustic fluctuation can again be spatially decomposed as

$$\rho_0 \widetilde{u_{0i}{}'^{\tau} u_{0j}{}'^{\tau}}^{t} = \overline{\rho_0}^{t} (\widetilde{\overline{u_{0i}{}'^{\tau}}^{x} \overline{u_{0j}{}'^{\tau}}^{x}}^{t} + \widetilde{u_{0i}{}'^{\tau\prime x} u_{0j}{}'^{\tau\prime x}}^{t} + \widetilde{\overline{u_{0i}{}'^{\tau}}^{x} u_{0j}{}'^{\tau\prime x}}^{t} + \widetilde{u_{0i}{}'^{\tau\prime x} \overline{u_{0j}{}'^{\tau}}^{x}}^{t}) \qquad (13)$$

where the $\sim^t$ refers to Favre-averaging with respect to the integral time scale. In the above, the first term is the ARS. The last term refers to turbulent fluctuations below the acoustic time scale. This can be combined with the TRS term above the acoustic time scale referred to earlier, to form the full TRS to be modelled conventionally. The middle two refer to TAI terms, which need to be modelled newly.

A combustor containing a backward facing step for flame stabilization with fuel injection at the step corner is considered (Fig. 1). The shaded region of length h is considered for the flow computations, whereas the full length of the combustor L is considered for the acoustic computation. In the laminar regime, air-flow Reynolds number based the step height and inlet average velocity in the range of 292-2924 is considered in 2D. Four air-flow Reynolds numbers in the 9000-47000 range are simulated in the 3D turbulent regime, keeping the fuel flow rate constant. Turbulence in the flow is handled either by means of large eddy simulation (LES) and unsteady Reynolds-averaged Navier-Stokes (URANS) solution approach. In the former, the sub-grid scale (SGS) terms also including turbulence-acoustic interaction are simulated by adopting the monotonically implicit LES (MILES) approach [19]; a single step global chemical reaction is adopted with laminar finite-rate Arrhenius kinetics. In the latter, Reynolds shear stress (RSM) model is adopted for flow turbulence closure and finite-rate/eddy-dissipation model with 3-step chemistry is adopted for turbulence-chemistry interaction; the turbulence-acoustic interaction terms are ex-

plicitly identified and estimated based on the assumption of isotropic turbulence, from which the RMS component of turbulent velocity fluctuation is found. The TAI terms are modelled as the product of the RMS turbulent velocity fluctuation and the acoustic velocity in each direction. The acoustic damping is the only aspect that is modelled in an ad hoc fashion, and together with this, the strength of the dilatation source term driving the acoustics is artificially tuned to calibrate for acoustic amplitudes against the experimental data.

The 2D laminar flow simulations are performed with an in-house code based on the SIMPLE scheme. For the LES-acoustic coupled solutions, the flow computations are performed using the FASTEST3D code, extended in-house for consideration of temperature-dependent density and finite-rate chemistry. For the URANS-acoustic coupled solution, Ansys-Fluent 13 is used. All these flow solvers are coupled with CLAWPACK, for the acoustic simulation. The CLAWPACK code is modified for handling non-cuboidal geometry such as the internal backward-facing step considered in the present work. QSHEP is used for interpolating between the FASTEST3D and CLAWPACK mesh nodes in the LES-acoustic coupled solution, whereas MpCCI is used for interfacing between Ansys-Fluent 13 and CLAWPACK solvers in the URANS-acoustic coupled simulations.

In both cases of LES and URANS, the flow and acoustic codes and their coupling are systematically benchmarked under cold flow and reacting flow conditions against available data.

3 Results and Discussion

The first part of this section is devoted to computations in the time domain. A few variations are explored on the 2D model problem to gain understanding. The evolution of the flow length scale h during the coupled simulation is first analysed, with the acoustic damping switched off. The flow length scale is identified with the extent of the flame; its variation is captured by plotting the parameter n, the exponent defined to relate the ratio of length-scales to the small parameter ϵ (refer to Section 2). Approach of n towards unity signifies the approach of the flow and acoustics towards a single time scale. Figure 2 shows the evolution of n for Re in the range of 292-2924, after the flame and acoustic fields are coupled (at $t > 6$). Increasing the inlet air velocity into the combustor decreases the flow time scale through the combustion zone and makes it approach the acoustic time scale. As the inlet air velocity increases, the starting value of n obviously increases, but its sharp growth towards unity occurs much sooner in the evolution of the flow-acoustic coupling. The simulations are stopped when the acoustic velocity increases to the same order as that of the flow velocity. This is because acoustic damping is not included in the above formulation.

Considering acoustic attenuation limits the growth of acoustic amplitude as expected. Figure 3 shows the acoustic pressure monitored at the mid-y location of the inlet duct along the step plane. In the absence of acoustic attenuation, the acoustic field grows indefinitely. With the action of ARS and inlet plane perturbation, the base-flow velocity also increases, and the coupled system could only be computed to capture the system's near-time behaviour. However, with acoustic attenuation, long-time behaviour of the coupled system could be computed. After an initial decay (spanning over a few acoustic cycles), the amplitude of the acoustic pressure increases sharply, due to a corresponding increase in the base flow divergence. As the coupled system is allowed to evolve in time, considerable vortex/flame roll-up (Fig. 4 a, b) and shedding (Fig. 4c) is observed. Due to the action of ARS, small vortical structures are being formed and they concatenate (Fig. 4a) to form a larger vortical structure (Fig. 4b), which is subsequently shed from the step plane (Fig. 4c). These features are commonly observed in the operation of practical combustors and the coupled simulation based on the present formulation approximately accounting for acoustic attenuation is able to reproduce them.

The turbulent flow simulations are amenable to experimental comparison. Figure 5 shows the

dominant frequencies and amplitudes compared between the experimental and simulation results. The pressure amplitudes from the LES-acoustic coupled solution compare well with experimental data and the dominant frequencies compare very well except at low Reynolds numbers (Fig. 5). The ARS is observed to have a huge effect in causing the nonlinear rise in amplitude, capturing the combustion instability phenomenon, as in the experimental observations.

The URANS-acoustic simulations show unsteady shear layer behaviour with acoustic coupling when compared to a relatively steady state behaviour without the coupling, but the damping to the large-scale vortex roll-up provided by the turbulence model in the flow hinders obtaining the amplitude trends correctly (Fig. 5). Consequently, the predicted frequency (Fig. 5) coincides with the duct natural mode at all Reynolds numbers, unlike in the experimental observations.

Figure 6 shows the heat release rate contours with the LES comparing the cases with and without the acoustic coupling with the incompressible flow at Re = 18000 and 33000. It can clearly be seen that the flame zone becomes very compact because of coupling with the acoustics, much more so when the time scales are closer together.

We now turn to the harmonic domain approach. In this approach, the most important aspect is the computation of the flame describing function, and this is the focus of the present paper. Most of the literature on this approach is reported for premixed flames. The present work on the backward facing step combustor with fuel injection at the step corner is thus not directly extended to perform the harmonic domain computations, particularly for want of experimental data for comparison. However, the approach is outlined with pertinent results of certain key steps.

We recognize the possibility of Helmholtz splitting [20] of the flow into the incompressible vortical component and compressible inviscid component, i.e., the acoustic velocity fluctuations. Accordingly, the velocity vector ν can be split into an irrotational part ν_{ir} and a rotational part v_r, such that the divergence in the flow field is contained in the irrotational part and all the vorticity is present in the rotational part, as given below:

$$\nu = \nu_{ir} + \nu_r \tag{14}$$

$$\bigtriangledown \bullet \nu = \bigtriangledown \bullet \nu_{ir} \tag{15}$$

$$\bigtriangledown \times \nu = \bigtriangledown \times \nu_r \tag{16}$$

Taking $\nu_{ir} = \bigtriangledown\psi$, where ψ is a scalar, the governing equation for the irrotational component in the presence of the flame is the Poisson equation in ψ, with the source as the divergence of the total velocity. Neumann boundary condition is specified at all the boundaries except at the exit plane. At the walls, the normal variation of ψ is taken as zero so as to satisfy the no-penetration condition. At the inlet plane, it is equated to the upstream velocity. At the exit plane, the second derivative of ψ in the axial direction has to be kept zero. However, with the streamlines straightening downstream of the flame, a Dirichlet boundary condition with $\psi = 0$ is adopted. With these and the source field obtained from the instantaneous total velocity field, the Poisson equation is solved by Fourier transform methods [21], and the irrotational velocity field is obtained. Figure 7 shows the total flow field, the irrotational flow field, and the rotational flow field obtained as a subtraction of the second from the first, for the backward facing step flow at Re = 200 that is externally excited at Strouhal number of 0.14 in one cycle.

When the flame is acoustically perturbed by external forcing, the acoustic propagation occurs along the irrotational flow streamlines shown in Fig. 7b. All the mass flux fluctuations in the flow are carried along these perturbations, leaving the vorticity fluctuations obtained as a difference between the total flow and the acoustic fluctuations as zero net-mass flux perturbations.

In the acoustically coupled simulations, the acoustic velocity fluctuations obtained by solving the acoustic equations can be applied as unsteady boundary conditions for the flow at the upstream boundary of the flow domain. The effect of this is shown in Fig. 8 in terms of three levels of initial amplitudes of acoustic velocity fluctuations as a fraction of the mean flow. The time evolution of the acoustic pressure in these cases clearly shows a strong effect of the inlet velocity amplitude, indicating the amplitude nonlinearity. As mentioned earlier, the damping kicks in when the amplitude grows significantly, and with vortex combustion downstream of the step, the pressure signal behaves like that of a kicked reactor, as mentioned by Sterling and Zukowski [22].

In the harmonic domain analysis, the irrotational velocity field as shown above (Fig. 7b) can be used for not only the inlet forcing, but also to compute the ARS to add to the momentum equation of the incompressible flow solver, to obtain the flame describing function. The combined effect of the inlet forcing and the ARS would result in the amplitude nonlinearity, to form the basis of constructing the flame describing function.

4 Conclusion

Much of the complexity in the modelling of the combustion instabilities is with regard to the flame zone. Full compressible simulations overdo the task by attempting to resolve the multiple length scales and time scales of the flow and the acoustic fields in different parts of the combustor simultaneously. Even when the flame zone alone is numerically simulated, considering that the flow field is of low mean Mach number, it would be advantageous to simulate incompressible flow equations, provided the proper effect of acoustics can be captured.

We recognize that the full compressible 3D unsteady Navier-Stokes equations for chemically reacting flow fields can be decomposed, up to first order, into incompressible flow equations governing the flame zone and acoustic wave equations governing the acoustic field overlaying the flame zone. These two equation sets are coupled by means of source terms, each evaluated from the solution to the other set. A basic formulation is presented in a generalized multi-time/multi-length scale framework, which can be adopted even under conditions when significant acoustic feedback does not affect the combustion process, leading to mere low-amplitude combustion noise from a typically turbulent flame zone, if the characteristic time scales of the flame and the acoustic processes are distinctly different. On the other hand, as conditions are varied for the two characteristic time scales to approach each other, flow-acoustic lock-on can be shown to occur, leading to onset of combustion instability. This formulation is general enough to be adopted for practical turbulent flows.

The formulation is extended to apply to LES and URANS approaches, and additional terms resulting from the flow-acoustic decomposition are identified for modelling. The results of dominant frequencies and amplitudes are compared against experimental data, and the comparison is quite reasonable. As expected, LES compares better than URANS, mainly because the turbulence model of the latter smears the formation of large eddies during excitation of high amplitude sound.

The approach to be adopted for harmonic domain computations is also outlined. Using the Helmholtz splitting theorem, the acoustic streamlines followed by the perturbations from the external acoustic forcing can be separately determined, from which the ARS is evaluated and added to the incompressible flow momentum equation for the computation of the flame describing function. Strong amplitude nonlinearity is observed because of the action of the ARS.

5 References

[1] S. C. Schadow, E. J. Gutmark, Prog. Energy Combust. Sci. 18 (1992) 117-132.

[2] T. C. Lieuwen, B. T. Zinn, Proc. Combust. Inst. 27 (1998) 18091816.

[3] S. Sivasegaram, J. H. Whitelaw, Combust. Sci. Technol. 52 (1987) 413-426.

[4] T. C. Lieuwen, J. Propul. Power 18 (2002) 61-67.

[5] S. R. Chakravarthy, O. J. Shreenivasan, B. Boehm, A. Dreizler, J. Janicka, J. Acoust. Soc. Am. 122 (1) (2007) 120-127.

[6] R. Balachandran, S. R. Chakravarthy, R. I. Sujith, J. Propul. Power 24 (6) (2008) 1382-1389.

[7] A. P. Dowling, S. R. Stow, J. Propul. Power 19 (5) (2003) 751-764.

[8] X. Wu, M. Wang, P. Moin, N. Peters, J. Fluid Mech. 497 (2003) 23-53.

[9] M. Tyagi, S. R. Chakravarthy, R. I. Sujith, Combust. Theo. Modell. 11 (2) (2007) 205-226.

[10] K. Balasubramaniam, R. I. Sujith, J. Fluid Mech. 594 (2008) 29-57.

[11] S. Roux, G. Lartigue, T. Poinsot, U. Meier, C. Brat, Combust. Flame 141 (2005) 40-54.

[12] L. Selle, L. Benoit, T. Poinsot, F. Nicoud, W. Krebs, Combust. Flame 145 (2006) 194-205.

[13] Y. Huang, V. Yang, Combust. Flame 136 (2004) 383-389.

[14] B. Muller, J. Eng. Math 34 (1998) 97-109.

[15] R. Klein, ESAIM:M2AN 39 (2005) 537-559.

[16] C. Balaji,S. R. Chakravarthy, AIAA-Paper No. 2010-26, American Institute of Aeronautics and Astronautics, Washington D.C. (2010).

[17] S. N. Rschevkin, "A Course of Lectures on the Theory of Sound", Mcmillan, NY, 1963.

[18] S. Temkin, "Elements of Acoustics", John Wiley and Sons, New York, 1981.

[19] F. F. Grinstein, L. G. Margolin, and W. J. Rider, Implicit large eddy simulation computing turbulent fluid dynamics. Cambridge 2007.

[20] W. Zdunkowski and A. Bott, Dynamics of atmosphere: a course in theoretical metereology. Cambridge University Press 2003.

[21] Press, W. H., S. A. Teukolsky, W. T. Vetterling, and B. P. Flannery, Numerical recipes in C: The art of scientific computing. 3rd ed. Cambridge University Press, 2007.

[22] Sterling, J. D. and Zukoski, E. E., Nonlinear dynamics of laboratory combustor pressure oscillations, Combust. Sci. Technol. 77, 225-238.

6 Figures

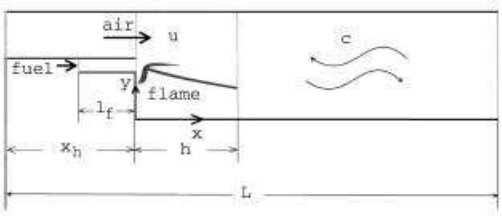

Figure 1: Schematic of the combustor.

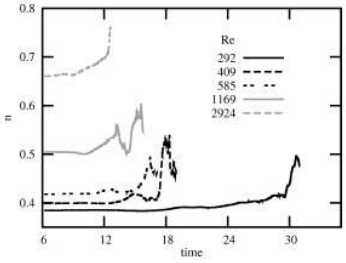

Figure 2: Evolution of n.

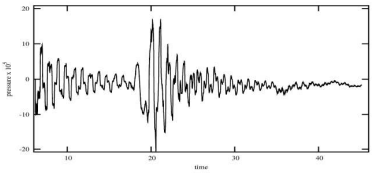

Figure 3: Evolution of acoustic pressure.

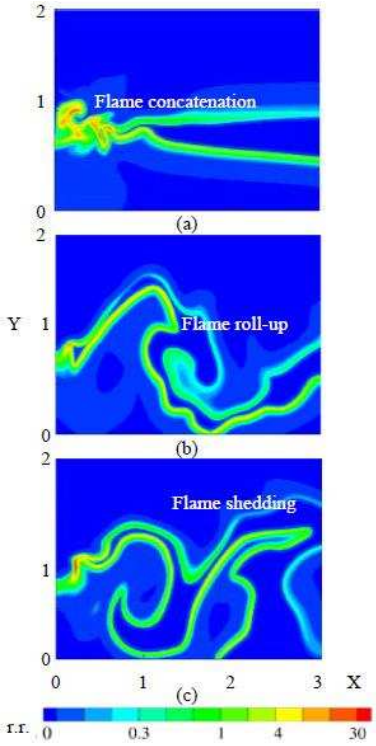

Figure 4: Evolution of flame acoustic coupled system. The figures are separated by 13 acoustic cycles. For explanation see text. X and Y are the Cartesian coordinate axes.

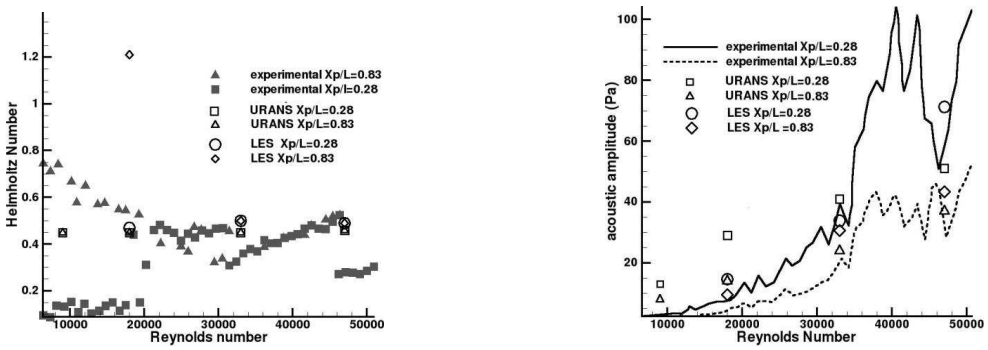

Figure 5: LES and URANS predictions of frequency and amplitude of acoustic pressure and comparison with experimental data.

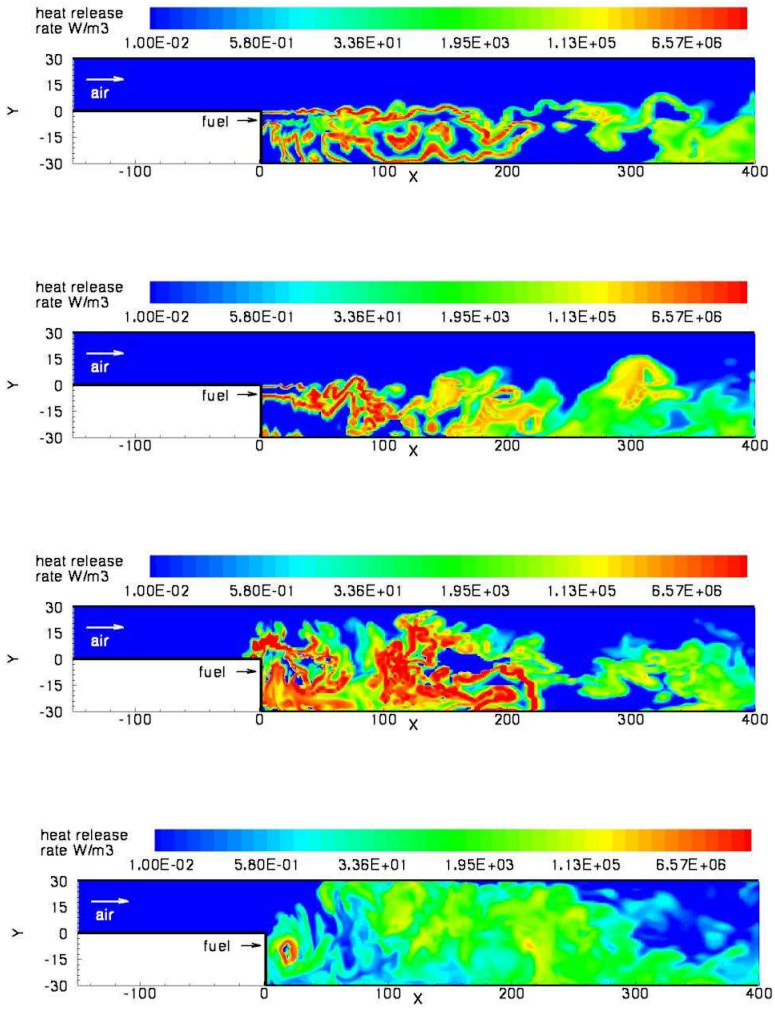

Figure 6: Comparison between acoustically uncoupled and coupled LES. (a) Uncoupled, Re = 18000, (b) Uncoupled, Re = 33000,(c) Coupled, Re = 18000, (d) Coupled, Re = 33000

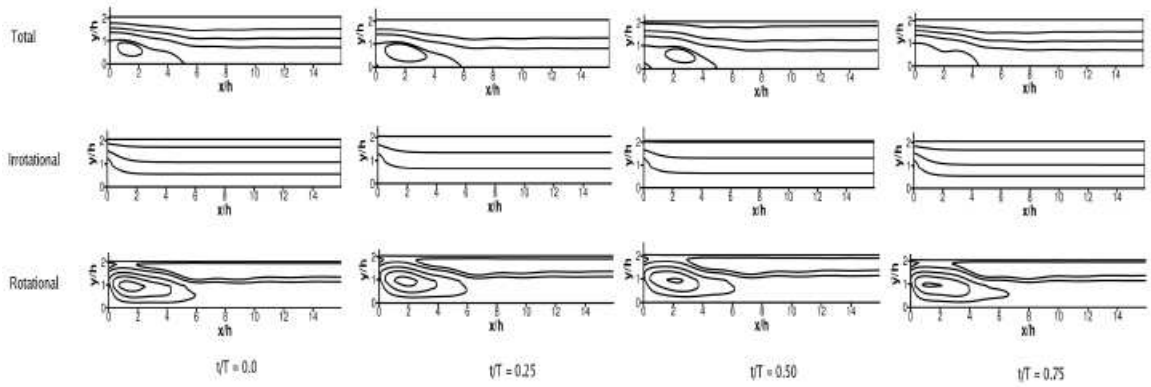

Figure 7: Streamlines of (a) total flow field, and its (b) irrotational and (c) rotational components.

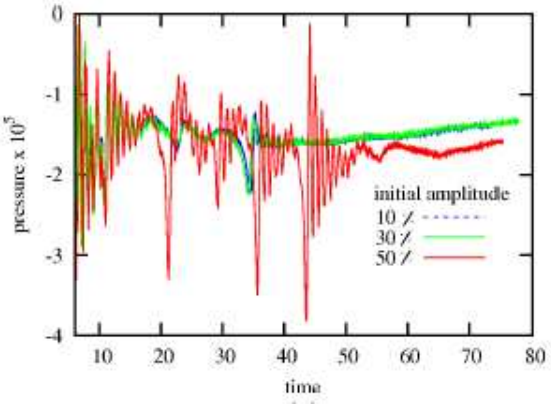

Figure 8: Effect of initial acoustic velocity amplitude on acoustic pressure evolution for Re = 585.